Advanced Materials Research Vol. 854 (2014) pp 29-34
© (2014) Trans Tech Publications, Switzerland
doi:10.4028/www.scientific.net/AMR.854.29

Acoustic phonon and surface roughness spin relaxation mechanisms in strained ultra-scaled silicon films

D. Osintsev[a,b], V. Sverdlov[a], and S. Selberherr[a]

[a] Institute for Microelectronics, TU Wien, Gußhausstraße 27–29 / E360, A–1040 Wien, Austria

[b] Volgograd State Technical University, Lenin Avenue 28, 400131 Volgograd, Russia

E-mail: {Osintsev|Sverdlov|Selberherr}@iue.tuwien.ac.at

Keywords: surface-roughness relaxation, phonon relaxation, ultra-scaled SOI MOSFETs, shear strain

Abstract: We consider the impact of the surface roughness and phonon induced relaxation on transport and spin characteristics in ultra-thin SOI MOSFET devices. We show that the regions in the momentum space, which are responsible for strong spin relaxation, can be efficiently removed by applying uniaxial strain. The spin lifetime in strained films can be improved by orders of magnitude, while the momentum relaxation time determining the electron mobility can only be increased by a factor of two.

Introduction

Future microelectronic devices should exhibit substantially reduced power consumption per operation. In addition, novel devices have to be smaller and faster. Spintronics considers novel devices which use the spin of electrons instead of the charge to perform an operation. A number of devices utilizing spin have already been proposed [1, 2]. Silicon is an ideal material for spintronic devices, because it is composed of nuclei with predominantly zero spin and is characterized by small spin-orbit coupling. Both factors tend to reduce spin relaxation. Understanding the details of the spin propagation in modern ultra-scaled silicon MOSFETs is urgently needed [3]. We present an approach to analyze surface roughness and phonon induced spin and momentum relaxation in thin silicon films. We investigate the dependences on temperature and uniaxial strain for different film thicknesses.

Model

We consider (001) oriented silicon films of thickness t. In order to find the scattering and spin relaxation matrix elements the subband wave functions and subband energies have to be known. A perturbative $\mathbf{k}\cdot\mathbf{p}$ approach [4–6] is suitable to describe the electron subband structure in the presence of strain and spin-orbit interaction. We consider only the two relevant valleys along the [001] axis. The Hamiltonian is written in the vicinity of the X-point along the k_z-axis in the Brillouin zone [7]. In order to find the subband wave functions and subband energies the Hamiltonian [7] is transformed to eliminate the coupling between the spins with opposite direction in different valleys:

$$H=\begin{bmatrix} \frac{\hbar^2k_z^2}{2m_l}+\frac{\hbar^2(k_x^2+k_y^2)}{2m_t}+U(z)-\delta & 0 & \frac{\hbar^2k_0k_z}{m_l} & 0 \\ 0 & \frac{\hbar^2k_z^2}{2m_l}+\frac{\hbar^2(k_x^2+k_y^2)}{2m_t}+U(z)-\delta & 0 & \frac{\hbar^2k_0k_z}{m_l} \\ \frac{\hbar^2k_0k_z}{m_l} & 0 & \frac{\hbar^2k_z^2}{2m_l}+\frac{\hbar^2(k_x^2+k_y^2)}{2m_t}+U(z)+\delta & 0 \\ 0 & \frac{\hbar^2k_0k_z}{m_l} & 0 & \frac{\hbar^2k_z^2}{2m_l}+\frac{\hbar^2(k_x^2+k_y^2)}{2m_t}+U(z)+\delta \end{bmatrix} \quad (1)$$

$U(z)$ is the confinement potential $\delta=\sqrt{\left(D\varepsilon_{xy}-\frac{\hbar^2k_xk_y}{M}\right)^2+\Delta_{SO}^2\left(k_x^2+k_y^2\right)}$, m_t and m_l are the transversal and the longitudinal silicon effective masses, $k_0=0.15\times2\pi/a$ is the position of the valley minimum relative to the X-point in unstrained silicon, ε_{xy} denotes the shear strain

component, $M^{-1} \approx m_t^{-1} - m_0^{-1}$, Δ_{SO}=1.27meVnm [4], and D = 14eV is the shear strain deformation potential. The same approach as for the two-band **k·p** Hamiltonian written in the vicinity of the *X*-point of the Brillouin zone for silicon films under uniaxial strain [6] is applicable to find the eigenfunctions and eigenenergies.

Spin and momentum relaxation rates are then calculated by thermal averaging in the following way [4, 8]:

$$\frac{1}{\tau} = \frac{\int \frac{1}{\tau(\mathbf{K_1})} f(\varepsilon)\left(1 - f(\varepsilon)\right) d\mathbf{K_1}}{\int f(\varepsilon)\, d\mathbf{K_1}} \tag{2}$$

$$f(\varepsilon) = \frac{1}{1 + \exp\left(\frac{\varepsilon - E_F}{k_B T}\right)} \tag{3}$$

$$\int d\mathbf{K_1} = \int_0^{2\pi} \int_0^{\infty} \frac{|\mathbf{K_1}(\varphi, \varepsilon)|}{\left|\frac{\partial \varepsilon(\mathbf{K_1})}{\partial \mathbf{K_1}}\right|} d\varphi\, d\varepsilon \tag{4}$$

ε is the electron energy, $\mathbf{K_1}$ is the in-plane wave vector, k_B is the Boltzmann constant, T is the temperature, and E_F is the Fermi level.

The intra- and intersubband surface roughness scattering matrix elements are taken proportional to the square of the product of the subband function derivatives at the interface [8]. The surface roughness at the two interfaces is assumed to be independent and described by a mean value and a correlation length. The surface roughness induced momentum (spin) relaxation rate is calculated in the following way:

$$\frac{1}{\tau_{SR}(\mathbf{K_1})} = \frac{2(4)\pi}{\hbar} \sum_{i,j=1,2} \int_0^{2\pi} \pi \Delta^2 L^2 \frac{1}{\epsilon_{ij}^2(\mathbf{K_2} - \mathbf{K_1})} \frac{\hbar^4}{4 m_l^2} \left[\left(\frac{d\Psi_{i\mathbf{K_1}\sigma}}{dz}\right)^* \frac{d\Psi_{j\mathbf{K_2}\sigma(-\sigma)}}{dz}\right]^2_{z=\pm\frac{t}{2}} \times \\ \times \exp\left(\frac{-(\mathbf{K_2} - \mathbf{K_1})^2 L^2}{4}\right) \frac{|\mathbf{K_2}|}{\left|\frac{\partial \varepsilon(\mathbf{K_2})}{\partial \mathbf{K_2}}\right|} \frac{1}{(2\pi)^2} d\varphi \tag{5}$$

ϵ_{ij} is the dielectric permittivity, L is the autocorrelation length, Δ is the mean square value of the surface roughness fluctuations, $\Psi_{i\mathbf{K_1}\sigma}$ and $\Psi_{j\mathbf{K_2}\sigma}$ are the wave vectors, and σ is the spin projection to the [001] axis.

The electron-phonon scattering induced momentum relaxation rates are evaluated in a standard way [8]. The intravalley spin relaxation due to transverse acoustic phonons is computed as:

$$\frac{1}{\tau_{TA}(\mathbf{K_1})} = \frac{\pi k_B T}{\hbar \rho v_{TA}^2} \sum \int_0^{2\pi} \frac{|\mathbf{K_2}|}{\left|\frac{\partial \varepsilon(\mathbf{K_2})}{\partial \mathbf{K_2}}\right|} \left| 1 - \frac{\frac{\partial \varepsilon(\mathbf{K_2})}{\partial \mathbf{K_2}} f(\varepsilon(\mathbf{K_2}))}{\frac{\partial \varepsilon(\mathbf{K_1})}{\partial \mathbf{K_1}} f(\varepsilon(\mathbf{K_1}))} \right| \times \\ \times \int_0^t \int_0^t \exp\left(-\sqrt{q_x^2 + q_y^2}|z - z'|\right) \left[\Psi_{\mathbf{K_2}\sigma}^\dagger(z) M \Psi_{\mathbf{K_1}-\sigma}(z)\right]^* \left[\Psi_{\mathbf{K_2}\sigma}^\dagger(z') M \Psi_{\mathbf{K_1}-\sigma}(z')\right] \times \\ \times \left[\sqrt{q_x^2 + q_y^2} - \frac{8 q_x^2 q_y^2 - \left(q_x^2 + q_y^2\right)^2}{q_x^2 + q_y^2} |z - z'|\right] dz dz' \tag{6}$$

ρ =2329$\frac{\mathrm{kg}}{\mathrm{m}^3}$ is the silicon density, v_{TA}=5300$\frac{\mathrm{m}}{\mathrm{s}}$ is the transversal phonons velocity, t is the film thickness, $(q_x, q_y) = \mathbf{K_1} - \mathbf{K_2}$, and M written in the basis for the spin relaxation rate is:

$$M = \begin{bmatrix} 0 & 0 & \frac{D_{xy}}{2} & 0 \\ 0 & 0 & 0 & \frac{D_{xy}}{2} \\ \frac{D_{xy}}{2} & 0 & 0 & 0 \\ 0 & \frac{D_{xy}}{2} & 0 & 0 \end{bmatrix} \tag{7}$$

D_{xy}=14eV is the shear strain deformation potential.

The intravalley spin relaxation rate due to the longitudinal acoustic phonons is calculated as:

$$\frac{1}{\tau_{LA}(\mathbf{K_1})} = \frac{\pi k_B T}{\hbar \rho v_{LA}^2} \sum \int_0^{2\pi} \frac{|\mathbf{K_2}|}{\left|\frac{\partial \varepsilon(\mathbf{K_2})}{\partial \mathbf{K_2}}\right|} \left| 1 - \frac{\frac{\partial \varepsilon(\mathbf{K_2})}{\partial \mathbf{K_2}} f(\varepsilon(\mathbf{K_2}))}{\frac{\partial \varepsilon(\mathbf{K_1})}{\partial \mathbf{K_1}} f(\varepsilon(\mathbf{K_1}))} \right| \times$$
$$\times \int_0^t \int_0^t \exp\left(-\sqrt{q_x^2 + q_y^2}|z - z'|\right) \left[\Psi_{\mathbf{K_2}\sigma}^\dagger(z) M \Psi_{\mathbf{K_1}-\sigma}(z)\right]^* \left[\Psi_{\mathbf{K_2}\sigma}^\dagger(z') M \Psi_{\mathbf{K_1}-\sigma}(z')\right] \times \tag{8}$$
$$\times \frac{4 q_x^2 q_y^2}{\left(\sqrt{q_x^2 + q_y^2}\right)^3} \left[\sqrt{q_x^2 + q_y^2}|z - z'| + 1\right] dz dz'$$

v_{LA}=8700$\frac{\mathrm{m}}{\mathrm{s}}$ is the speed of the longitudinal phonons.

The intervalley spin relaxation rate due to acoustic phonons contains the Elliot and Yafet contributions [3], which are calculated in the following way:

$$\frac{1}{\tau_{LA}(\mathbf{K_1})} = \frac{\pi k_B T}{\hbar \rho v_{LA}^2} \sum \int_0^{2\pi} \frac{|\mathbf{K_2}|}{\left|\frac{\partial \varepsilon(\mathbf{K_2})}{\partial \mathbf{K_2}}\right|} \left| 1 - \frac{\frac{\partial \varepsilon(\mathbf{K_2})}{\partial \mathbf{K_2}} f(\varepsilon(\mathbf{K_2}))}{\frac{\partial \varepsilon(\mathbf{K_1})}{\partial \mathbf{K_1}} f(\varepsilon(\mathbf{K_1}))} \right| \times$$
$$\times \int_0^t \left[\Psi_{\mathbf{K_2}\sigma}^\dagger(z) M' \Psi_{\mathbf{K_1}-\sigma}(z)\right]^* \left[\Psi_{\mathbf{K_2}\sigma}^\dagger(z) M' \Psi_{\mathbf{K_1}-\sigma}(z)\right] dz \tag{9}$$

The matrix M' is written as:

$$M' = \begin{bmatrix} D' & 0 & 0 & D_{SO}(q_y - iq_x) \\ 0 & D' & D_{SO}(-q_y - iq_x) & 0 \\ 0 & D_{SO}(-q_y + iq_x) & D' & 0 \\ D_{SO}(q_y + iq_x) & 0 & 0 & D' \end{bmatrix} \tag{10}$$

$\boldsymbol{D'}$=12eV, $\boldsymbol{D_{SO}}$=15meV/$\boldsymbol{k_0}$ [3], $\boldsymbol{k_0} = 0.15\times 2\boldsymbol{\pi}/\boldsymbol{a}$ is the position of the valley minimum relative to the X-point in unstrained silicon.

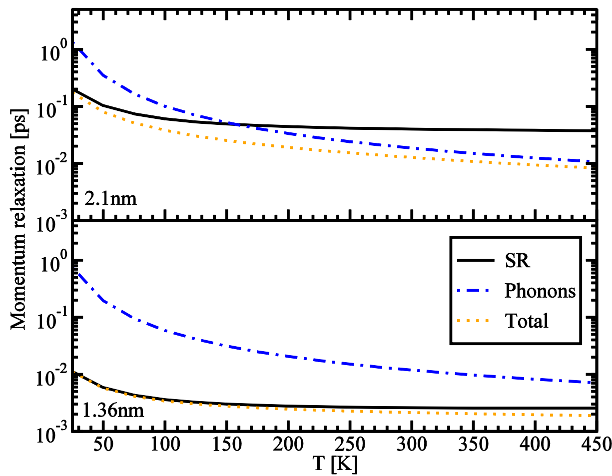

Figure 1: Dependence of the momentum relaxation time induced by surface roughness (SR), phonons, and total momentum relaxation time on temperature for two different thicknesses, ε_{xy}=0, and electron concentration $1.29{\cdot}10^{12}$ cm^{-2}.

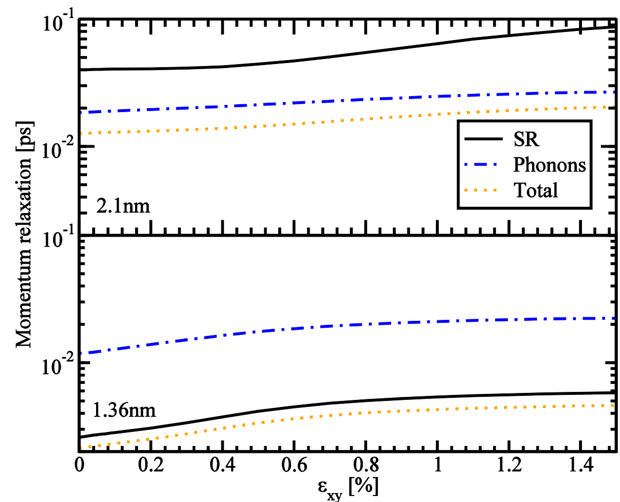

Figure 2: Dependence of the momentum relaxation time induced by surface roughness (SR), phonons, and total momentum relaxation time on shear strain for 1.36nm and 2.1nm film thicknesses, for T=300K, and electron concentration $1.29{\cdot}10^{12}$ cm^{-2}.

Results and Discussion

Figure 1 shows the dependence of the momentum relaxation time on temperature. The contributions from the surface roughness (SR) and phonons to the total momentum relaxation time are shown. The phonon contribution to the total relaxation time depends strongly on temperature. Thus, for the film thicknesses 2.1nm and 1.36nm, the surface roughness is the dominant mechanism of the momentum relaxation at low temperatures. For a temperature around 150K for the film of 2.1nm thickness the surface roughness induced and phonon induced momentum relaxation mechanisms yield similar contributions to the total relaxation time. At room temperature the total momentum relaxation time is mainly determined by phonon scattering. However, Figure 1 shows that for the thinner film the dominant relaxation mechanism is the surface roughness in the whole range of investigated temperatures. Thus, the dominant relaxation mechanism strongly depends on the film thickness. Indeed, the phonon limited momentum relaxation is characterized by a weaker thickness dependence and does not increase as significantly as the surface roughness induced relaxation, when the thickness is decreased from 2.1nm to 1.36nm. The surface roughness limited momentum relaxation increases by more than an order of magnitude because of the expected t^{-6}dependence [8, 9]. Thus, for the thickness 1.36nm the surface roughness induced spin relaxation is the dominant mechanism for the whole range of considered temperatures.

Figure 2 shows the dependence of the different mechanisms of the momentum relaxation together with the total momentum relaxation time on shear strain. The improvement of the momentum relaxation time due to the shear strain is around 60% for the film thickness of 2.1nm and around 110% for the film thickness 1.36nm. The phonons limited momentum relaxation time improves by around 45% for 2.1nm and 90% for 1.36nm. The surface roughness limited momentum relaxation time increases by 120% for 2.1nm and for 1.36nm. Because the surface roughness mechanism is the dominant for the film thickness 1.36nm, the increase of the total momentum relaxation time is higher for 1.36nm than for 2.1nm film thickness. We point out that the increase of the momentum relaxation time is due to the corresponding scattering matrix elements dependences on strain. Combined with the strain induced effective mass decrease it should result in an even better mobility improvement supporting the use of uniaxial tensile strain as the mobility booster in fully depleted ultra-thin SOI MOSFETs.

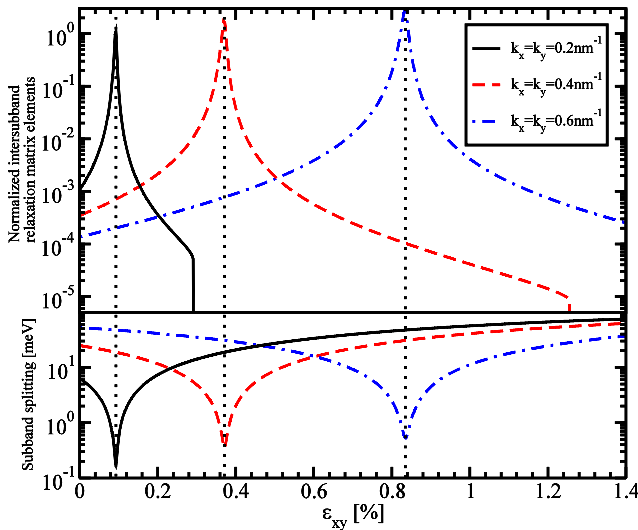

Figure 3: Normalized intersubband relaxation matrix elements and subband splitting as a function of shear strain for different values of the wave vectors.

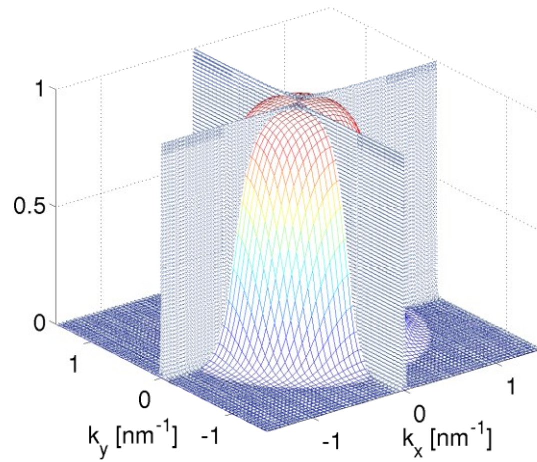

Figure 4: Intersubband relaxation matrix elements normalized to the intrasubband scattering elements at zero strain for an unstrained sample. The Fermi distribution for 300K is also shown.

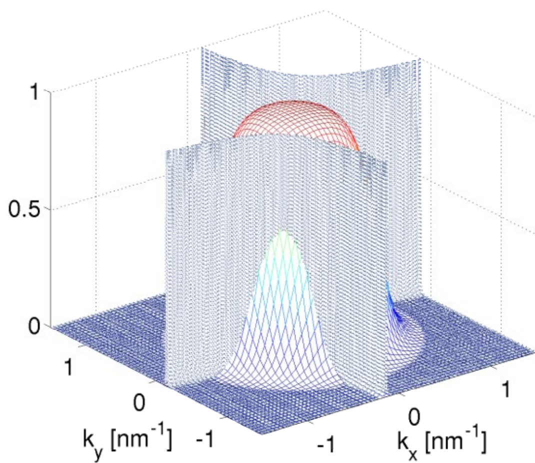

Figure 5: Normalized intersubband relaxation matrix elements for shear strain 0.5% shown together with the Fermi distribution at 300K.

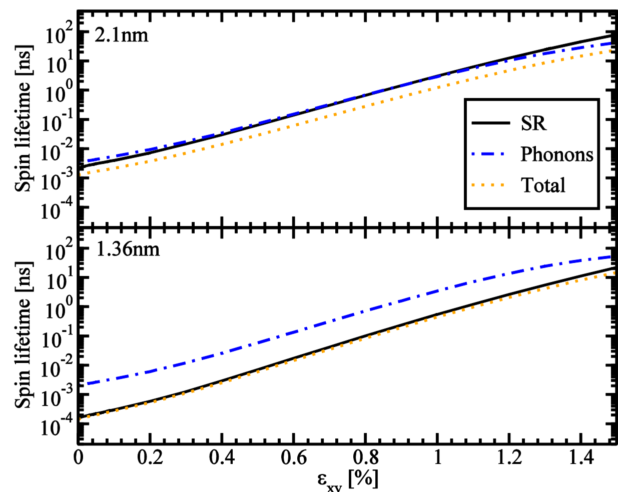

Figure 6: Dependence of the spin lifetime induced by surface roughness (SR), phonons, and total momentum relaxation time on shear strain for two different film thicknesses, for T=300K, and electron concentration $1.29\cdot10^{12}$ cm^{-2}.

Figure 3 shows the energy splitting within the lowest unprimed subband (the "valley splitting") induced by the confinement and the bulk dispersion non-parabolicity. The surface roughness spin relaxation matrix elements normalized to the scattering matrix elements at zero strain as a function of shear strain are also shown. To evaluate the electron spin relaxation we take the matrix elements on the wave functions with the opposite spin projections $\sigma' = -\sigma$ corresponding to the spin flip events. Normalized spin relaxation matrix elements display sharp peaks at the same values of strain, where the intersubband splitting is reduced. These minima are determined by the condition $D\varepsilon_{xy} - \frac{\hbar^2 k_x k_y}{M} = 0$. At these points the splitting between the subbands is determined only by the spin-orbit term. Under this condition the spin-orbit interaction leads to a large mixing between the spin-up and spin-down states from the opposite valleys, resulting in the "hot spots" formation characterized by strong spin relaxation.

Figure 4 displays the normalized spin relaxation matrix elements for an unstrained film. The "hot spots" are along the [100] and [010] directions. Shear strain pushes the "hot spots" to higher energies (Figure 5) outside of the states occupied by carriers. This leads to a reduction of the spin relaxation.

A strong increase of the spin lifetime with shear strain at room temperature is demonstrated in Figure 6. The surface roughness and phonon contributions to the total spin lifetime are shown. For the film of 2.1nm thickness the surface roughness induced spin relaxation is of the same order as the phonon contribution. However, for the film of 1.36nm thickness the phonon contribution is about an order of magnitude weaker compared to the surface roughness induced spin relaxation. Importantly, the spin relaxation caused by both phonons and surface roughness increases by orders of magnitude with shear strain of 1.5% applied. Thus, uniaxial stress is an efficient tool to boost the spin lifetime in ultra-thin SOI MOSFETs.

Conclusion

By utilizing the **k·p** approach which included the spin-orbit interaction effects we found the subband wave functions and subband energies in (001) thin silicon films. We have shown that the momentum relaxation time can be improved by almost a factor of two for ultra-thin films. We have demonstrated a strong, several orders of magnitude, increase of spin lifetime in strained silicon films. Thus shear strain used to boost mobility can also be used to increase spin lifetime.

Acknowledgment

This work is supported by the European Research Council through the grant #247056 MOSILSPIN. The computational results have been achieved using the Vienna Scientific Cluster (VSC).

References

[1] S. Sugahara and J. Nitta, Spin transistor electronics: An overview and outlook, Proc. of the IEEE, 98(12) (2010) 2124–2154.

[2] S. Datta and B. Das, Electronic analog of the electro-optic modulator, Applied Physics Letters 56 (1990) 665-667.

[3] Y. Song, H. Dery, Analysis of phonon-induced spin relaxation processes in silicon, Phys. Rev. B 86 (2012) 085201.

[4] P. Li, H. Dery, Spin-orbit symmetries of conduction electrons in silicon, Phys. Rev. Lett. 107 (2011) 107203.

[5] G.L. Bir, G.E. Pikus, Symmetry and strain-induced effects in semiconductors. New York / Toronto: J. Wiley & Sons, 1974.

[6] V. Sverdlov, Strain-induced effects in advanced MOSFETs. Wien - New York. Springer, 2011.

[7] D. Osintsev *et al.*, Reduction of surface roughness induced spin relaxation in MOSFETs by strain, Proc. of the Int. Workshop on Computational Electronics (2012).

[8] M.V. Fischetti *et al.*, Six-band k·p calculation of hole mobility in silicon inversion layers: Dependence on surface orientation, strain, and silicon thickness, Journ. of Appl. Phys. 94 (2003) 1079-1095.

[9] S. Jin, M.V. Fischetti, T.-W. Tang, Modeling of surface roughness scattering in ultrathin-body SOI MOSFETs, IEEE Trans. Electron Devices 54(9) (2007) 2191–2202.